Grant number: FA9550-15-1-0105

Research Title: An observational and modelling study of upwelling in the auroral thermosphere

PI: Anasuya L. Aruliah

Period of performance: 1st February 2015 - 31st January 2016

REPORT DOCUMENTATION PAGE

Form Approved OMB No. 0704-0188

1. REPORT DATE *(DD-MM-YYYY)*
28/04/2016

2. REPORT TYPE
Final performance report

3. DATES COVERED *(From - To)*
01/02/2015-31/01/2016

4. TITLE AND SUBTITLE
An observational and modelling study of auroral upwelling in the thermosphere

5a. CONTRACT NUMBER
FA9550-15-1-0105

5b. GRANT NUMBER

5c. PROGRAM ELEMENT NUMBER

6. AUTHOR(S)
Aruliah, Anasuya, L.,

5d. PROJECT NUMBER

5e. TASK NUMBER

5f. WORK UNIT NUMBER

7. PERFORMING ORGANIZATION NAME(S) AND ADDRESS(ES)
University College London
Gower Street, London, WC1E 6BT, UK

8. PERFORMING ORGANIZATION REPORT NUMBER

9. SPONSORING/MONITORING AGENCY NAME(S) AND ADDRESS(ES)
European Office of Aerospace Research and Development(EOARD)
86, Blenheim Crescent, Ruislip, Middlesex HA4 7HB, UK

10. SPONSOR/MONITOR'S ACRONYM(S)
EOARD

11. SPONSOR/MONITOR'S REPORT NUMBER(S)

12. DISTRIBUTION/AVAILABILITY STATEMENT
Distribution A - Approved for Public Release

13. SUPPLEMENTARY NOTES

14. ABSTRACT
This is a study of the importance of the altitude of energy deposition for causing upwelling of the upper atmosphere. Observations in the auroral regions of Scandinavia, in parallel with a modelling study, are presented. Independent measurements of the thermosphere were made using Fabry-Perot Interferometers, and of the ionosphere over a range of altitudes (100-600km) using the EISCAT and KAIRA radars. The CMAT2 simulations augment the Carlson et al. [2012] simulations that successfully replicated the doubling of thermospheric density at the cusp observed by the CHAMP satellite [Lühr et al., 2004]. The Carlson mechanism was tested qualitatively by investigating whether similar upwelling was observed in the auroral region, and could be supported by model simulations. Both dayside cusp and nightside auroral regions have large electric fields generated by either dayside or nightside magnetic reconnection, respectively. The experiments and model simulations show that the manifestation of heating in the density changes and structure of the upper atmosphere is complex. The location of the heat source, whether due to soft or hard particle precipitation, is one aspect, but the location with respect to the magnetospheric dynamo is also critically important.

15. SUBJECT TERMS
thermosphere, airglow, neutral winds, density

16. SECURITY CLASSIFICATION OF:			17. LIMITATION OF ABSTRACT	18. NUMBER OF PAGES	19a. NAME OF RESPONSIBLE PERSON
a. REPORT	b. ABSTRACT	c. THIS PAGE			19b. TELEPHONE NUMBER *(Include area code)*

AFRL-AFOSR-UK-TR-2016-0013

Upwelling Auroral Thermosphere 150105

Anasuya Aruliah
UNIVERSITY COLLEGE LONDON

05/05/2016
Final Report

DISTRIBUTION A: Distribution approved for public release.

Air Force Research Laboratory
AF Office Of Scientific Research (AFOSR)/ IOE
Arlington, Virginia 22203
Air Force Materiel Command

Table of Contents

List of Figures

List of Tables

Summary

Introduction

Methods, Assumptions and Procedures

Results and Discussion

Conclusions

References

List of Symbols, Abbreviations and Acronyms

Summary

This is a study of the importance of the altitude of energy deposition for causing upwelling of the upper atmosphere. Observations in the auroral regions of Scandinavia, in parallel with a modelling study, are presented. Independent measurements of the thermosphere were made using Fabry-Perot Interferometers, and of the ionosphere over a range of altitudes (100-600km) using the EISCAT and KAIRA radars. The CMAT2 simulations augment the *Carlson et al.* [2012] simulations that successfully replicated the doubling of thermospheric density at the cusp observed by the CHAMP satellite [*Lühr et al.*, 2004]. The Carlson mechanism was tested qualitatively by investigating whether similar upwelling was observed in the auroral region, and could be supported by model simulations. Both dayside cusp and nightside auroral regions have large electric fields generated by either dayside or nightside magnetic reconnection, respectively. The experiments and model simulations show that the manifestation of heating in the density changes and structure of the upper atmosphere is complex. The location of the heat source, whether due to soft or hard particle precipitation, is one aspect, but the location with respect to the magnetospheric dynamo is also critically important.

Introduction

One of the frequently cited papers within the past decade for upper atmospheric research has been the CHAMP satellite finding by *Lühr et al.* [2004] of a near doubling of the thermospheric density over the geomagnetic cusp region. This was a localised and persistent feature that covered a horizontal distance of only a few hundred kilometres. A density enhancement greater than 1.2 times the background level was seen in ~50% of the observations when CHAMP crossed the cusp, and even more frequently with the GRACE satellite at a higher orbit of 480 km altitude [*Kervalishvili and Lühr*, 2013].

The density anomaly observed by CHAMP has important repercussions for the satellite industry. Predicting satellite orbits, and their lifetimes, relies on realistic atmospheric drag models, which requires an understanding of the mechanisms that cause the anomaly.

Although the perturbation in the cusp density covers a small region of the polar region, it is a persistent effect that will systematically slow down satellites. This will affect the many important polar orbiting satellites used for research, industry and the military. By identifying and understanding the mechanism it will be possible to predict other regions where density anomalies are likely to exist, or to develop under certain geophysical conditions.

Atmospheric density decreases exponentially with altitude owing to gravity. The increased density observed by the CHAMP satellite orbiting at 400 km altitude is likely to be the result of upwelling of denser air from below. Several mechanisms that cause the upwelling have been proposed, supported by model simulations, but no definitive conclusions have been reached. For this EOARD grant we proposed an observational experiment in the auroral midnight region to test the models. With two previous EOARD grants we undertook midday cusp region experiments in January 2012 and January 2013 using the UCL Fabry-Perot Interferometer (FPI) and Scanning Doppler Imager (SCANDI) at Svalbard to measure the thermospheric neutral winds and temperatures, with the EISCAT Svalbard Radar (ESR) measuring ionospheric parameters in the same volume of atmosphere. Using this grant, we measured the neutral thermosphere and ionosphere in the midnight auroral region. The EISCAT radars in Tromsø, Norway, and the KAIRA VHF radar array in Kilpisjarvi, Finland, were used to measure the ionosphere. The UCL FPIs at the Kiruna ESRANGE Optical Platform Site (KEOPS) site near Kiruna, Sweden, and at the Sodankylä Geophysical Observatory, Finland, measured the neutral gas simultaneously over a small region of the auroral oval for two 6 hour periods around magnetic midnight (2100UT) near new moon in February 2015.

Results related to this study have been presented at the following conferences:

European Geophysical Union conference (April 2015)
A.L. Aruliah, A. Ronksley, D. Johnson and H.C. Carlson, “Multi-instrument and modelling study of small-scale upwelling and density changes in the auroral thermosphere-ionosphere region”

National Astronomy Meeting (July 2015)
A. Ronksley and A.L.Aruliah, “Extreme Vertical Winds in the Thermosphere: Polar cap vs. Auroral Oval”
R. Hood and A.L.Aruliah, “Differences in satellite to ground-based wind measurements - modelling viscosity as a possible source”

A paper is in preparation, to be submitted to the peer-reviewed journal Annales Geophysicae:

A.L.Aruliah, A.Ronksley, D.Johnson, R.Hood, T.C.Spain, I.McWhirter, H.C.Carlson, “An observational and modelling study of upwelling in the auroral thermosphere”

Methods, Assumptions and Procedures

Figure 1 is a model simulation using the University College London (UCL) Coupled Middle Atmosphere Thermosphere (CMAT2) model [*Carlson et al., 2012*]. The plot shows the density enhancement above 300 km altitude between 70-80° N. The dotted line illustrates the path of the CHAMP satellite orbit at an altitude of 400 km. Figure 2 shows a simulation from a new empirical model of the electromagnetic energy (Poynting flux) input to the northern polar region above 60°N [*Cosgrove et al.*, 2014]. The paths of the UCL FPIs at Svalbard and KEOPS/Sodankylä as the Earth rotates under the auroral oval are shown by yellow and red dotted circles, respectively. The cusp region is shown by the bright red spot. The increased density in the cusp is associated with the upwelling of denser gas from below.

Figure 1: CMAT2 simulation of cusp upwelling and the doubling of density observed by the CHAMP satellite at 400 km (black dotted line). (taken from Carlson et al., 2012)

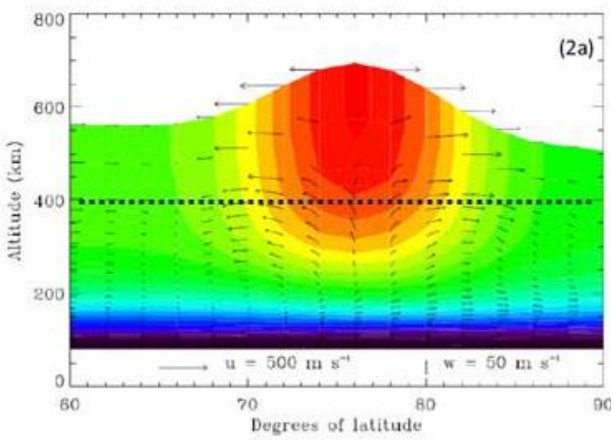

The arrows in Figure 1 illustrate the neutral wind speeds, where the magnitude of the wind is represented by the length of the arrow. The vertical component of the wind is expected to be small (up to 20 ms^{-1}) and short-lived due to hydrostatic equilibrium and the large viscosity of the thermosphere. The latter characteristic is expected to produce large temporal and spatial scale sizes of hours and a few thousand kilometres, respectively, for thermospheric structures. In other words, there is not much variation expected over a large volume of gas. Furthermore, a great deal of energy would be required to lift the gas, and increase its gravitational potential energy. However, over the last 20 years, there have been observations of strong vertical winds in the auroral regions that contradict the theoretical assumption of small vertical winds. Such observations have been achieved with the increasing sensitivity of detectors used with Fabry-Perot Interferometers (FPIs) [e.g. *Aruliah and Rees,* 1995; *Larsen and Meriwether*, 2012]; but large vertical winds are infrequent since hydrostatic equilibrium generally prevails. Vertical wind observations are typically made using narrow field-of-view FPIs, with a

Figure 2: A new Poynting flux empirical model for low geomagnetic activity using the FAST satellite

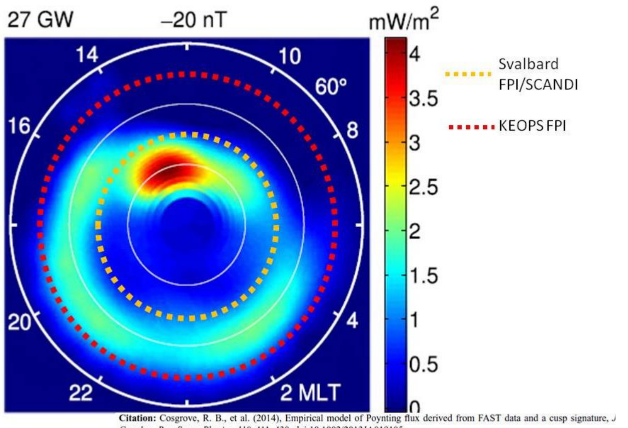

Citation: Cosgrove, R. B., et al. (2014), Empirical model of Poynting flux derived from FAST data and a cusp signature, *J Geophys. Res. Space Physics*, *119*, 411–430, doi:10.1002/2013JA019105.

sequence of different look directions lasting 10-15 minutes. Thus large vertical winds may appear as single measurements within one cycle. Our experiment uses multiple short exposure vertical look directions in order to follow the upwelling, and thereby verify that it is real by the consistency of successive measurements. Now that we are aware that large vertical winds occur, we expect to see more experiments optimised to look for them.

Figure 3 The fields of view of the KEOPS and Sodankylä FPIs are shown by a yellow and pink circle respectively. The green triangle shows the location of three sample volumes at 240 km altitude. The top left green dot represents the vertical Tromsø radar beam.

The Atmospheric Physics Laboratory at University College London (UCL) operates a network of Fabry-Perot Interferometers (FPIs) at three observatories in Arctic Scandinavia. The FPIs are located near each of the EISCAT incoherent scatter radars. Two of the observatories are in the region of the auroral oval, while the third is on Svalbard, in the polar cap. We have already carried out two radar-FPI experiments in the midday cusp sector of the polar cap (SP-UK-CUSP in January 2012 and SP-UK-CUSPN in January 2013). Using this grant we carried out a field trip to run a radar-FPI experiment in the magnetic midnight sector of the auroral oval region, which experiences very different geophysical conditions. UCL worked in collaboration with colleagues at EISCAT, KAIRA and the Sodankylä Geophysical Observatory/University of Oulu to make ground-based measurements of both the ionosphere and neutral gas component of the upper thermosphere in the auroral regions. We have the additional advantage of being able to use a physics-based model, the UCL CMAT2 model, to test these mechanisms.

The FPIs are at two sites near Kiruna, Sweden and Sodankylä, Finland, which are about 250 km kilometres apart as shown in Figure 3. The yellow circle defines the field-of-view of the Kiruna FPI, while the pink circle (which overlaps the yellow circle) defines the Sodankylä FPI. The FPIs made bistatic measurements of the properties of the uncharged (neutral) gas at two common volumes observed by both FPIs, shown by the bottom green dot and right hand green dot. The EISCAT radar at Tromsø measured the properties of the ionosphere all along a vertical column above the Tromsø radar, between altitudes 100-600 km, which is indicated by the top left green dot. The three EISCAT radars made tristatic measurements of a volume of atmosphere at 240 km above

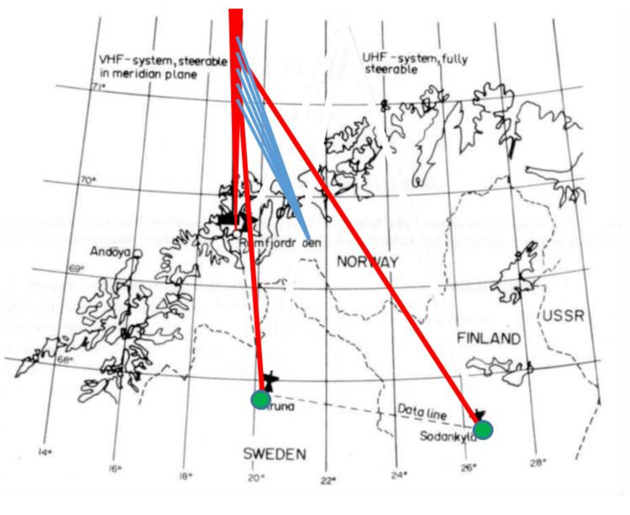

Figure 4 Bistatic VHF measurements along the vertical column above Tromsø using the 3 EISCAT radars and KAIRA multi-beam radar. Also shown are the 2 FPIs at Kiruna and Sodankylä (green dots).

Tromsø. Tristatic line-of-sight velocity measurements were combined to create the plasma velocity vectors from which electric fields and Joule heating can be calculated. The corners of the green triangle define the locations of the three volumes, at an altitude of 240km, which can be measured either bi-statically by FPIs or tri-statically by the EISCAT radars.

The experimental campaign to KEOPS was from Tuesday 3 Feb to Thursday 12 Feb 2015. The travel and subsistence, plus consultancy of the engineer in the field team, was funded by this grant. The team consisted of Dr Ian McWhirter (consultant opto-electrical engineer), Ms Amy Ronksley (who passed her PhD viva during the period of this project in December 2015 under the supervision of Dr Aruliah) and Dr Anasuya Aruliah (PI-permanent staff salary funded by UCL). Full calibration was carried out for the red and green line FPIs at KEOPS. This included repair of the motor that drives the pointing mirror for the green line FPI; re-parallelising the etalon plates for both FPIs; dealing with a sticky shutter on the green line FPI; re-sealing the window enclosing the etalon; some other minor repairs; and clearing snow from the roof to allow free view for the optical domes. A new cloud monitor, bought with this grant, was attached to the outside of the hut and set up under the control of the green line pc. Subsequently a 6th form student carried out a summer work experience project in July-August 2015 and determined that a clarity level > 35/50 matched with clear skies seen on the UCL all-sky camera. The cloud monitor will allow a more automatic identification of cloudy weather conditions. Presently we have relied on checking the all-sky camera for every night, which is very time-consuming.

Twelve hours of EISCAT radar time were awarded to Dr Aruliah for this experiment. This is equivalent to £18,000 for the cost of operation to the Natural Environment Research Council (NERC). The EISCAT-FPI campaign was scheduled for a 6 hour period around magnetic midnight (1800-0000UT) on each of the nights of 15 and 17 February 2015. The Kilpisjärvi Atmospheric Imaging Receiver Array (KAIRA) provided additional line-of-sight VHF radar measurements along the beam of the EISCAT Tromsø radar in order to determine plasma velocities bi-statically in the altitude range 150-200km (McKay-Bukowski et al., 2015). The KAIRA operation was funded by the Infrastructure Funds of the University of Oulu, Finland, and European Union funds as a technology pathfinder for EISCAT-3D (a European three-dimensional imaging radar for atmospheric and geospace research).

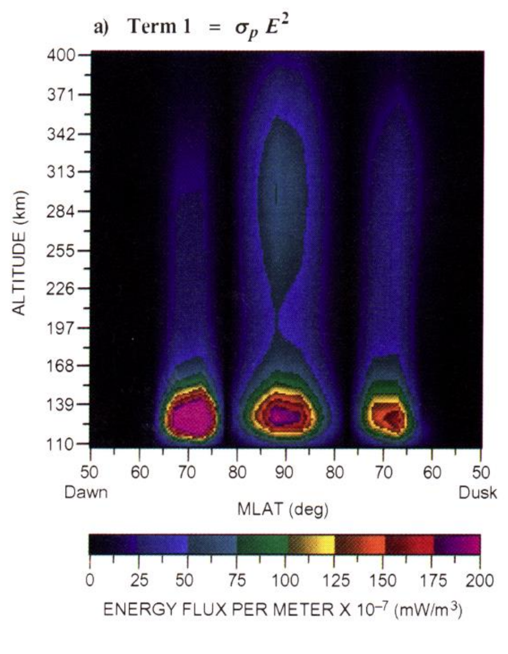

Figure 5 Conventional Joule heating in the region 110-150 km (Thayer et al., 1995)

In parallel to the FPI-EISCAT measurements, we ran simulations using the UCL Coupled Middle Atmosphere Thermosphere model (CMAT2), which is a 3-dimensional global circulation model of the Earth's middle and upper atmosphere, between 15-500km altitude. It solves the non-linear equations of energy, momentum and continuity on a model grid of 2° latitude, 18° longitude and 1/3 scale height. It includes thermospheric heating, photodissociation, and photoionisation based on solar fluxes,

absorption and ionisation cross-sections given by external models such as the Schumann-Runge continuum. Amongst other drivers CMAT2 includes chemistry and transport, and high latitude electric fields and particle precipitation models. A more detailed description may be found in Harris et al. (2002) and the references therein. The CMAT2 model simulations were carried out by PhD student David Johnson, who was funded for 3 months under this grant. Additional studies were carried out by PhD student Rosie Hood (funded under a UCL studentship).

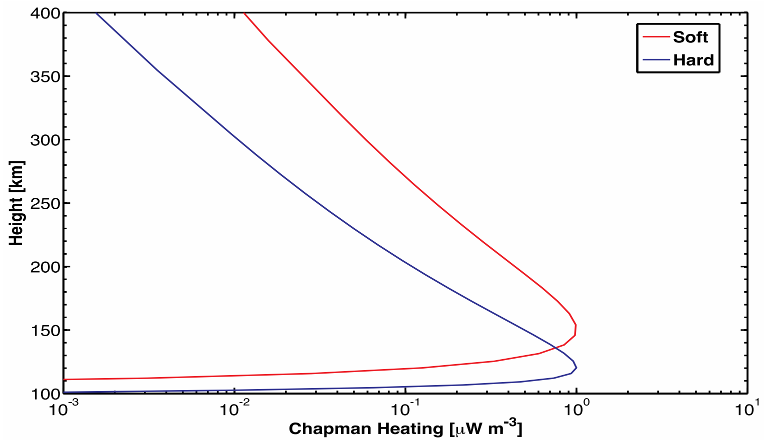

Figure 6 CMAT2 model simulation of soft (red line) and hard (blue line) precipitation.

Conventional modelling studies have the largest electrical conductivities, and consequently Joule heating, in the altitude region 110-150km, as demonstrated by Figure 5 from Thayer et al. (1995). Demars and Schunk (2007) demonstrated that it would require 110 times the heating power than has been observed to recreate the doubling of thermospheric density seen by CHAMP. So the CMAT2 simulations made by Carlson et al. (2012) were achieved by depositing energy over a height region representative of soft electron precipitation of a few keV energy, as shown by the red line in Figure 6; with the blue line representing hard precipitation representative of conventional model studies. The Carlson et al (2012) heating represented large electric fields typical of plasma velocities of 2,000-3,000 m/s, which is at the extreme end of observed plasma flow velocities. However, the mechanism of soft precipitation and fast plasma flows from reconnection was successfully demonstrated. The average density increase over the cusp is only 1.33 times the surrounding density rather than double (Kervalishvili and Lühr, 2013), and so more frequently observed values of plasma velocities are also capable of producing average density increases.

For this project we repeated the Carlson et al. (2012) model, and added to it three more simulations, thus creating 4 model scenarios for comparison as shown in Table 1. The heating is applied at a constant level for 1 hour, with a 10 minute linear warming up and cooling down before and after. The heating is centred on magnetic midday for Svalbard (0900 UT) and magnetic midnight for Kiruna (i.e. 2100 UT). The simulations are for January solar minimum, using f10.7 value of 80 and quiet steady state conditions.

Table 1: Four CMAT2 simulations of thermospheric heating

	Soft precipitation	Hard precipitation
Magnetic noon cusp	1	2
Magnetic midnight auroral oval	3	4

Model 1 reproduces the Carlson et al simulation. Model 2 represents the standard Joule heating scenario presented by Demars and Schunk (2007). Models 3 and 4 are the new studies to test the mechanism proposed by Carlson et al (2012) in the auroral midnight zone.

Results and Discussion

Figure 7 shows the CMAT2 vertical wind frequency distribution for comparison with the FPI distributions. The CMAT2 standard deviation is less than ±2ms^{-1}. This emphasises the difference between direct FPI observations and a model that assumes hydrostatic equilibrium which severely suppresses large-scale convection. However, the frequency distributions from direct measurements of the vertical winds by FPIs at Svalbard (Figure 8) and Kiruna (Figure 9) show a much broader distribution. The standard deviation for Svalbard is ±10 ms^{-1}, and is even broader for Kiruna at ±24 ms^{-1}. Both distributions are leptokurtotic, which means that they are close to being Gaussian (see the solid line on each graph), but are dominated by low values, so predominantly hydrostatic in behaviour.

Figure 10 shows the CMAT2 neutral temperatures (Tn) for the four simulations. The top plot shows the magnetic midday Svalbard Tn for the control simulation (dotted line) for soft (green line) and hard (red line) precipitation at 0900 UT, and then 1 hour later for soft (dashed green line) and hard (dashed red line) to show how the temperature relaxes quickly back to the background as heat is dissipated in all directions. It is dramatically apparent that soft precipitation is far more effective in heating the top of the thermosphere than hard. The top plot for Figure 11 shows the corresponding increases in Svalbard thermospheric densities. There is a 50% increase in density for the soft precipitation, but only about 10% increase with hard.

The response of the Kiruna neutral temperatures and densities for a 1 hour addition of heating at magnetic midnight (bottom plots of Figures 10 and 11) are significantly different. As with Svalbard the soft precipitation is more effective than hard; but the increases are small, and almost insignificant. This would imply that any upwelling and density increases in the region of the magnetic midnight sector of the auroral oval will be small. Indeed, the lack of reports of density anomalies by the CHAMP and other satellites, seem to support this contention.

Figure 12 shows the observations from 2nd night of observations on the 17th February 2015. The Kiruna FPI measurements of vertical winds are shown in the middle plot. The vertical winds varied between ±30 ms^{-1}. Both up-welling (20:10-20:20 UT; 22:40-22:25 UT) and down-welling (19:45-20:40 UT; 22:50-23:20 UT) were seen. The vertical winds corresponded to periods of soft and hard precipitation as shown by the top plot of EISCAT radar electron densities. The bottom plot shows the EISCAT ion temperatures. Bursts of heating are shown by ion temperatures reach values greater than 1500 K around 21:00 UT, 21:20 UT, 21:50 UT, 22:20 UT and 23:30 UT. Figure 13 shows the KAIRA determination of plasma velocities from combining line-of-sight measurements with the EISCAT vertical beam. Up until 21:00 UT fast westward plasma velocities of several hundred ms^{-1} throughout the height region 150-200km. From 21:50-21:50 UT there appears to be a reversal to northward followed by a predominantly southward flow until the end of observations at 23:00 UT. The combination of the electron densities and plasma flows determine the Joule heating, which we are

currently working on calculating. There are clearly bursts of reconnection in the magnetotail that are heating the ions. There is a fairly rapid response of the neutral atmosphere, which results in the up and down-welling seen by the FPI. The range of the vertical winds is beyond the standard deviation seen in the average Kiruna vertical winds shown in Figure 9.

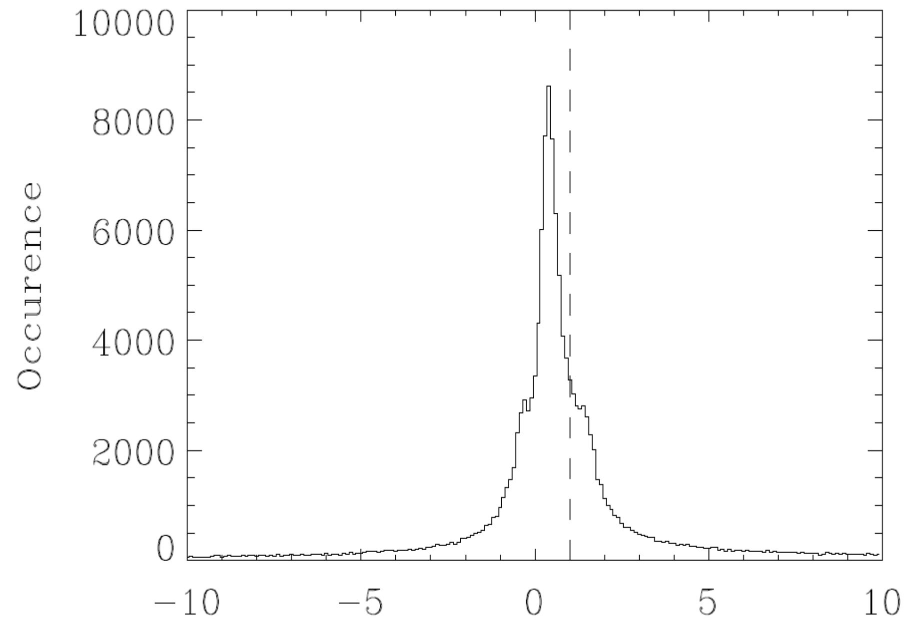

Figure 7 CMAT2 frequency distribution of vertical winds in m/s

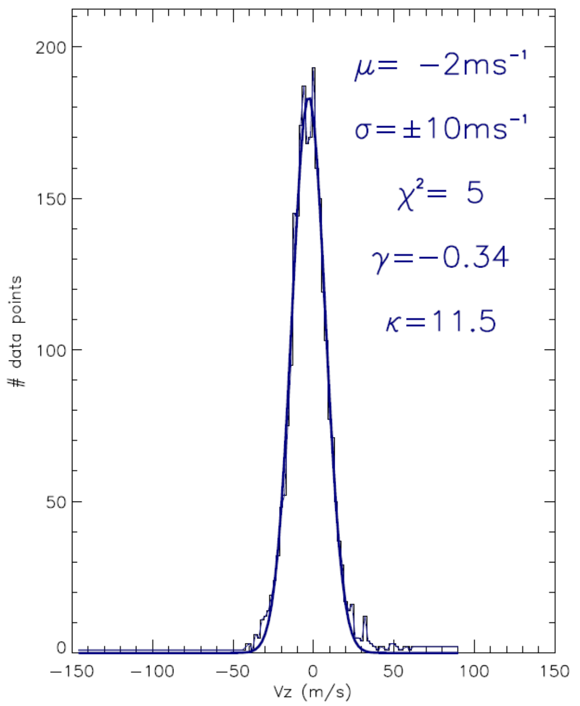

Figure 8 Svalbard vertical winds distribution

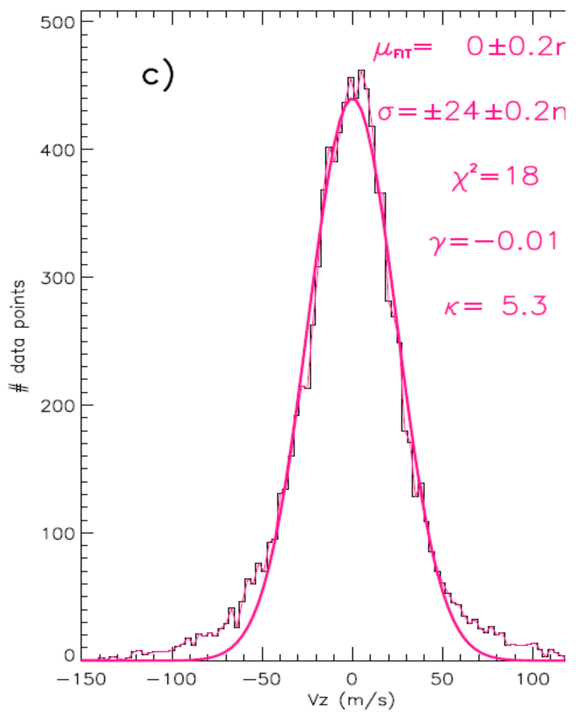

Figure 9 KEOPS FPI vertical wind distribution

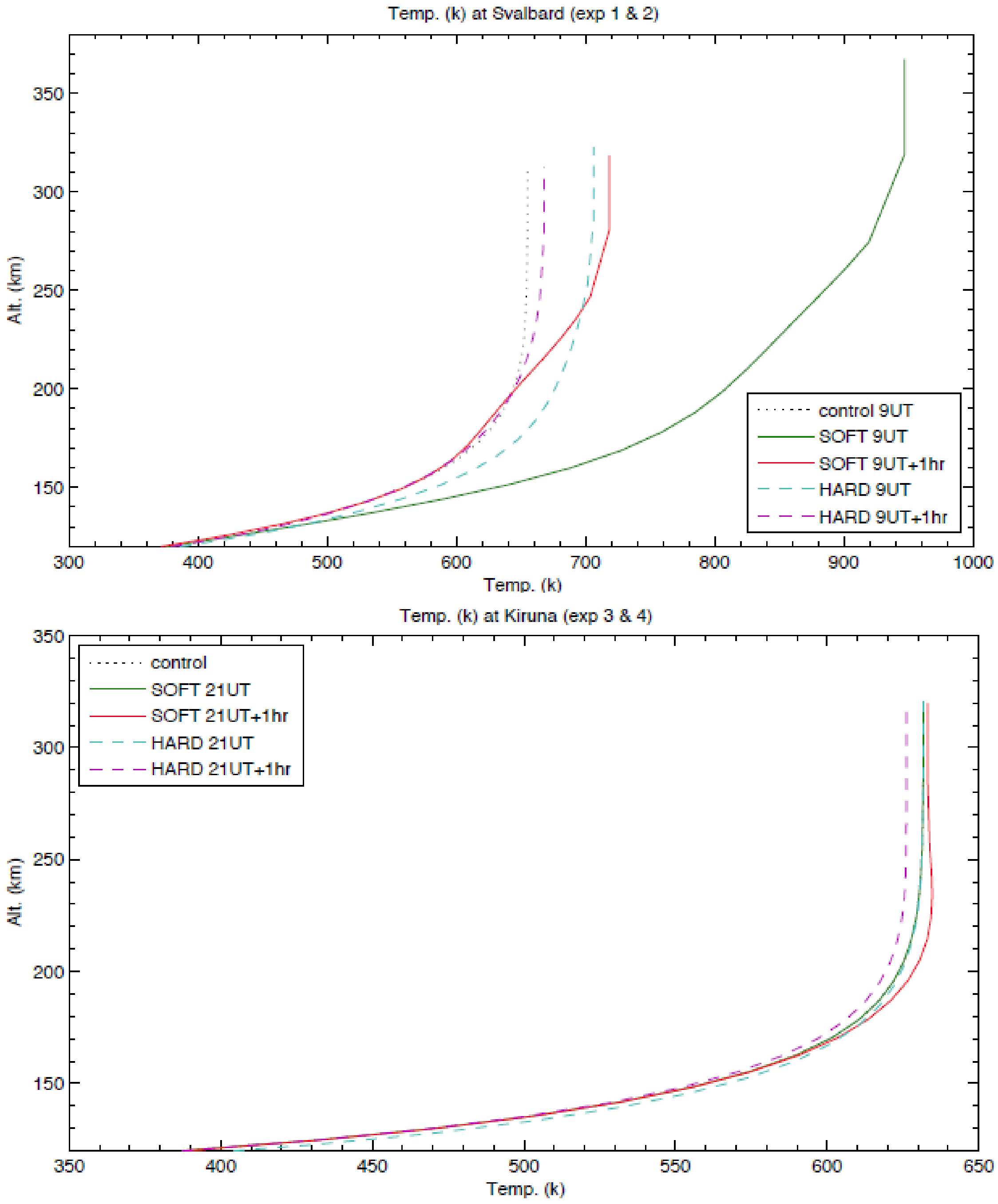

Figure 10 CMAT2 variation of neutral temperature with altitude at time of initial injection of heating and 1 hour afterwards. Top: Svalbard magnetic noon + 1 hour later simulations. Bottom: Kiruna magnetic midnight + 1 hour.

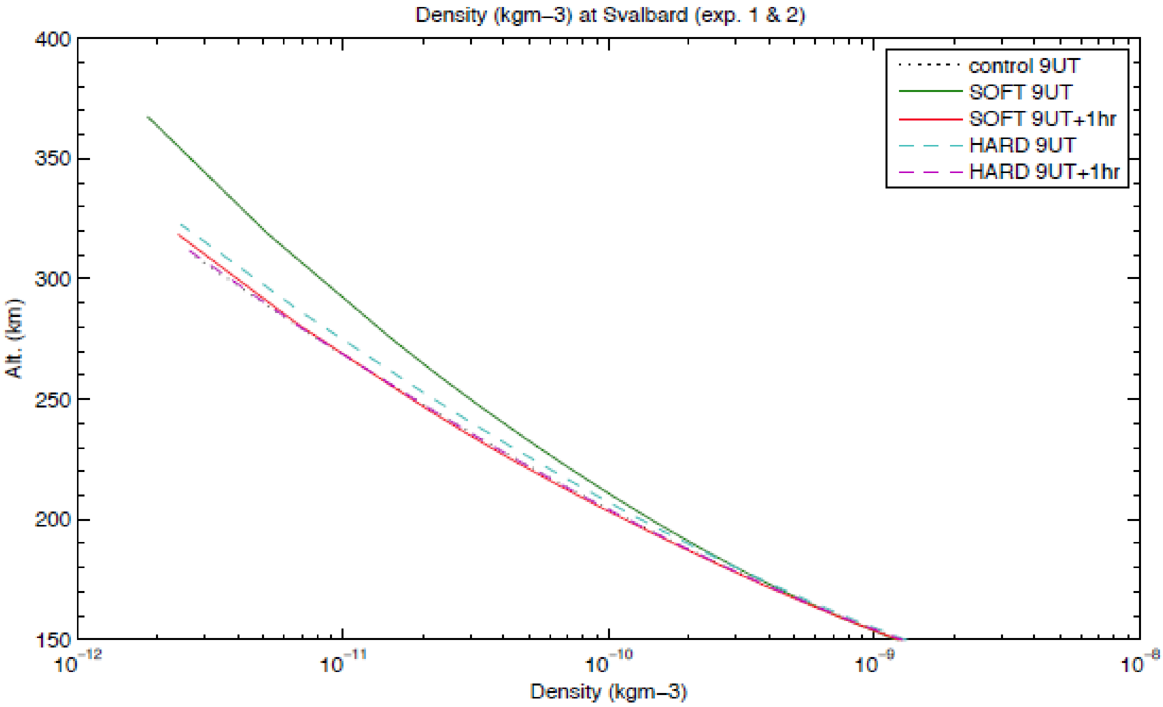

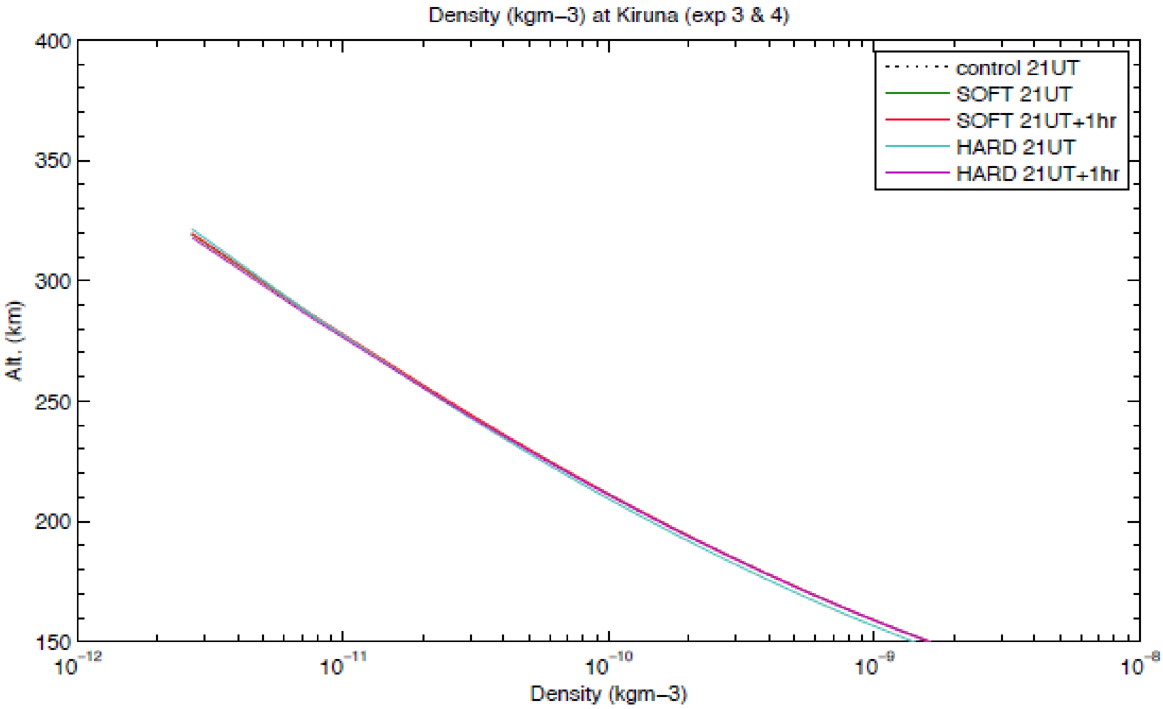

Figure 11 CMAT2 variation of thermospheric density with altitude at time of initial injection of heating and 1 hour afterwards. Top: Svalbard magnetic noon + 1 hour. Bottom: Kiruna magnetic midnight + 1 hour.

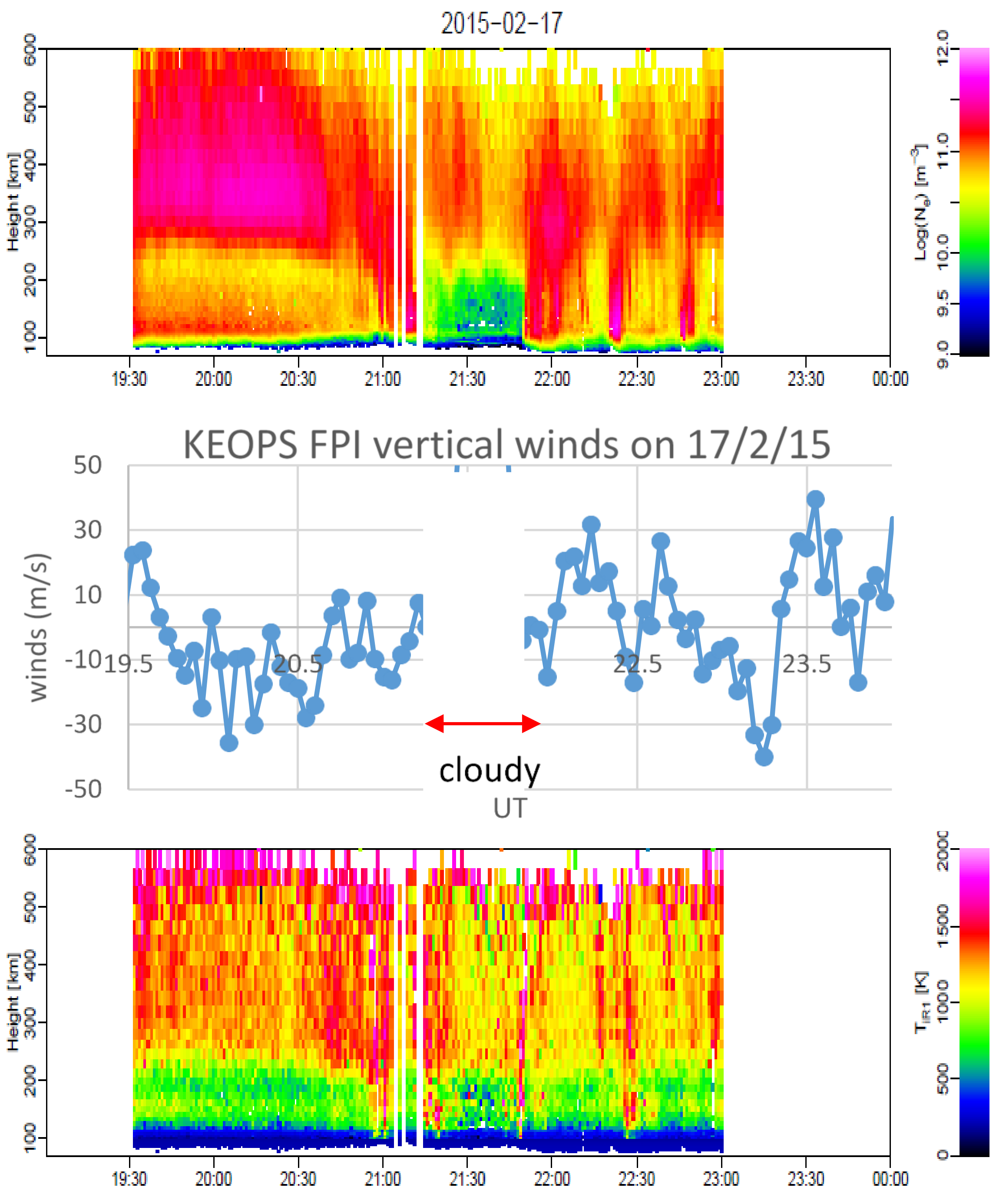

Figure 12 a) EISCAT radar electron densities. b) KEOPS vertical winds; c) EISCAT ion temperatures 1930-2300 UT on 17 February 2015.

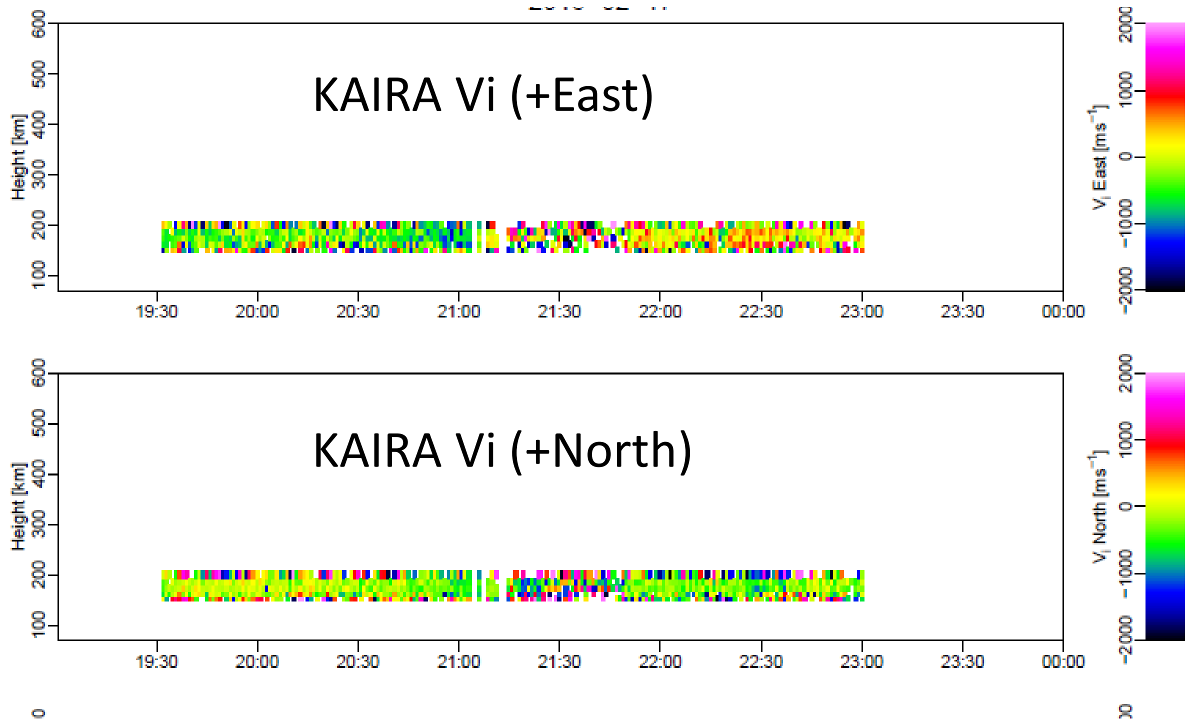

Figure 13 KAIRA horizontal plasma velocity components. Top Zonal (+ East) and bottom Meridional (+North)

Conclusions

The CMAT2 model study clearly demonstrates that Joule heating associated with soft particle precipitation results in a significantly larger thermospheric density at the top of the thermosphere. The four simulations show that heating in the midday cusp is significantly large for both soft and hard precipitation, but has a small effect in the midnight auroral region.

The CMAT2 model simulations complement observations made with FPIs and EISCAT radars. Svalbard FPI observations of the midday cusp sector from two earlier campaigns showed large vertical winds (several tens of ms^{-1} up to 200 ms^{-1}) that were consistent with the large density increases reported from CHAMP satellite measurements. These up-wellings occurred at the same time as soft particle precipitation and large plasma flows measured by the ESR radar, resulting in enhanced Joule heating in the expected altitude region of around 150-200 km. The new experiment funded by this grant measured vertical winds at Kiruna, when in the magnetic midnight zone of the auroral oval. The FPI measured vertical wind values ranged between ± 30 ms^{-1}, which is considerably larger than expected from non-hydrostatic models such as CMAT2. Up- and down-welling was seen. These moderately large vertical winds occurred during periods of large F-region electron density and plasma flows of the order of 1000 ms^{-1} as measured bi-statically using the EISCAT Tromsø radar and the KAIRA VHF radar array.

The experiments and model simulations show that the manifestation of heating in the density changes and structure of the upper atmosphere is complex. The location of the heat source, whether due to soft or hard particle precipitation, is one aspect, but the location with respect to the magnetospheric dynamo is also critically important.

References

Aruliah A.L., D.Rees, The Trouble with Thermospheric Vertical Winds: Geomagnetic, Seasonal and Solar Cycle Dependence at High Latitudes, J.Atmos.Terr.Physics, 57, 597-609, 1995 (special issue on vertical winds)

Aruliah, A.L., E.M.Griffin, A.D.Aylward, E.A.K.Ford, M.J.Kosch, C.J.Davis, V.S.C.Howells, E.Pryce, H.Middleton, J.Jussila, First direct evidence of meso-scale variability on ion-neutral dynamics using co-located tristatic FPIs and EISCAT radar in Northern Scandinavia, EISCAT workshop special issue Annales Geophys., 23, 147-162, 2005

Carlson, H. C., T. Spain, A. Aruliah, A. Skjaeveland, and J. Moen (2012), First-principles physics of cusp/polar cap thermospheric disturbances, Geophys. Res. Lett., 39, L19103, doi:10.1029/2012GL053034

Cosgrove, R. B., et al. (2014), Empirical model of Poynting flux derived from FAST data and a cusp signature, J.Geophys. Res. Space Physics,119, 411–430, doi:10.1002/2013JA019105.

Demars, H. G., R. W. Schunk, (2007), Thermospheric response to ion heating in the dayside cusp, J. Atmos. Sol. Terr. Phys, 69, 649-660.

Deng, Y., T.J.Fuller-Rowell, A.J.Ridley, D.Knipp, R.E.Lopez, (2013), Theoretical study: Influence of different energy sources on the cusp neutral density enhancement, 118, 2340-2349

Kervalishvili, G. N. and H. Lühr, (2013) The relationship of thermospheric density anomaly with electron temperature, small-scale FAC, and ion up-flow in the cusp region, as observed by CHAMP and DMSP satellites, Ann. Geophys., 31, 541–554, www.ann-geophys.net/31/541/2013/doi:10.5194/angeo-31-541-2013

Lühr, H., M. Rother, W. Köhler, P. Ritter, L. Grunwaldt, (2004), Thermospheric up-welling in the cusp region: Evidence from CHAMP observations, Geophys. Res. Lett., 31, 6, L06805, 10.1029/2003GL019314.

Larsen, M. F., and J. W. Meriwether (2012), Vertical winds in the thermosphere, J. Geophys. Res., 117, A09319, doi:10.1029/2012JA017843.

McKay-Bukowski, Derek, Juha Vierinen, Ilkka I. Virtanen, Richard Fallows, Markku Postila, Thomas Ulich, Olaf Wucknitz, Michiel Brentjens, Nico Ebbendorf, Carl-Fredrik Enell, Marchel Gerbers, Teun Grit, Peter Gruppen, Antti Kero, Toivo Iinatti, Markku Lehtinen, Henri Meulman, Menno Norden, Mikko Orispää, Tero Raita, Jan Pieter de Reijer, Lassi Roininen, Arno Schoenmakers,
Klaas Stuurwold, and Esa Turunen, KAIRA: The Kilpisjärvi Atmospheric Imaging Receiver Array—System Overview and First Results, IEEE TRANSACTIONS ON GEOSCIENCE AND REMOTE SENSING, VOL. 53, NO. 3, 2015

Ronksley, Amy, Optical remote sensing of mesoscale thermospheric dynamics above Svalbard and Kiruna, PhD thesis, UCL, 2016

Thayer, J.P., J.F.Vickrey, R.A.Heelis, J.B.Gary, Interpretation and modelling of the high-latitude electromagnetic energy flux, JGR, 100, 19715-19728, 1995

List of Symbols, Abbreviations and Acronyms

CMAT2	Coupled Middle Atmosphere Thermosphere model
EISCAT	European Incoherent Scatter Radar
ESR	EISCAT Svalbard Radar
FPI	Fabry Perot Interferometer
KAIRA	Kilpisjärvi Atmospheric Imaging Receiver Array
KEOPS	Kiruna ESRANGE Optical Platform Site
SCANDI	Scanning Doppler Imager
Te	Electron temperatures
Ti	Ion temperatures
Tn	Thermospheric neutral temperatures
UCL	University College London
Un	Thermospheric neutral winds
Vi	Ionospheric plasma speeds